Development of Highly Efficient Magnetic Bearing and Application to Ultra-Low Temperature Fluid Pump

Yohji Okada[a], Hironari Suzuki[a], Ken-ichi Matsuda[a], Ryou Kondo[a], and Masato Enokizono[b]

[a] Ibaraki University, Nakanarusawa 4-12-1, Hitachi, Ibaraki Pref. 316-8511 Japan, y.okada@mx.ibaraki.ac.jp
[b] Oita University, Dannoharu 700, Oita, Oita Pref. 870-1192, Japan

***Abstract*— Highly efficient hybrid type magnetic bearing is proposed in this paper. It is intended to apply the proposed magnetic bearing to ultra low temperature fluid pump. Traditional low temperature pump is supported by a ceramic ball bearing which is damaged by the low temperature liquid. Non-contact support is highly requested. However, the standard electro-magnetic bearing consumes high electric power causing heat to the liquid. This paper proposes highly efficient hybrid type radial magnetic bearing which can operate with very low power consumption. Also the pump is canned by the FRP pipe which has thick wall to separate the stator from the liquid. The designed magnetic bearing has 3 [mm] wide air gap with high force factor.**

I. INTRODUCTION

Traditional ultra-low temperature pump uses seramic ball bearing in the liquid. Hence there are several problems of short bearing life time, polution of powdered ceramic and heart transfer to the liquid.

The standard electro-magnetic bearing consumes high electric power and is not applicable [1]. In this paper highly efficient magnetic bearing is proposed for supporting the pump in ultra-low temperature liquid. A centrifugal pump is supported by a hybrid (HB) type radial magnetic bearing and the shaft is set in vertical position as shown in Fig. 1. The top of the shaft is supported by a standard ball bearing and motor, since the low temperature liquid is under this level. The stator of HB magnetic bearing is better to be separated from the fluid. A FRP pipe can be used in such a low temperature which has thick wall of 2 [mm] thickness [2]. The designed magnetic bearing has 3 [mm] wide air gap with high force factor [3]-[9]. Highly efficient magnetic bearing is realized by using strong bias flux produced by wide area neodymium permanent magnet (PM) and high cupper ratio coils by using pressed winding technology made by Selco Co., Ltd. [10].

II. HIGHLY EFFICIENT MAGNETIC BEARING

Principle of the proposed magnetic bearing is shown in Fig. 2. The stator has four main poles with pressed coil windings. Between them sub-poles are arranged which has strong and wide area neodymium PMs to produce high bias flux as shown by the solid black lines. The upper and lower control windings are connected series. To produce upward force the current of two coils are flown as shown by the arrow symbols which produce the dotted red control flux lines. This increases the upper air gap flux while decreases the lower air gap flux causing upward force as shown by the big blue arrow. Similar control is applied to the left and right coil windings to control the left and right direction. Hence the radial two directions are actively controlled.

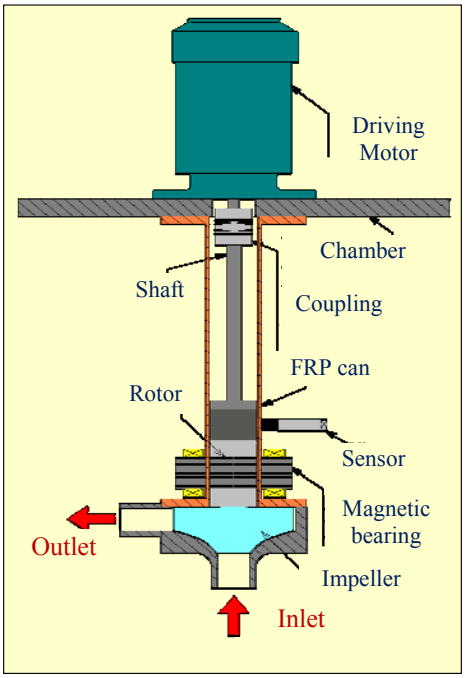

Figure 1. Ultra-low temperature fluid pump

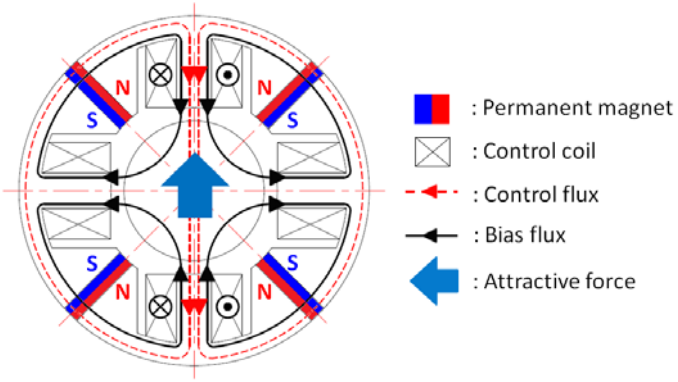

Figure 2. Principle of proposed radial magnetic bearing

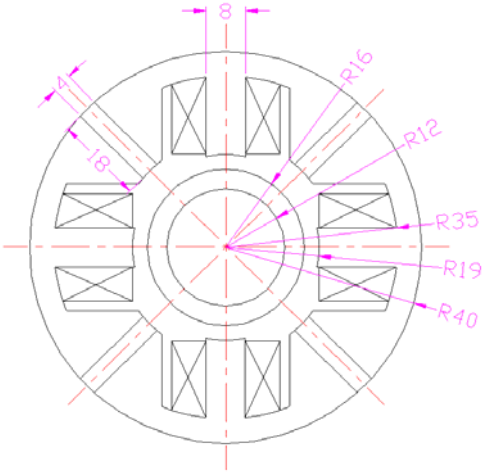

Figure 3. Analytical model

TABLE I PHYSICAL PARAMETERS

Item	Value, Material
Airgap	3 [mm]
Permanent magnet	Neodymium (NMX-48CH) ≒1000 [kA/m]
Coil turns	400 [turns/slot]
Core material	Electromagnetic silicon sheet 35A300

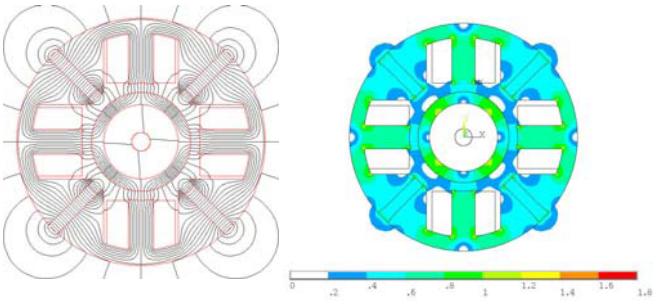

Figure 4. Bias flux lines and flux densities (Control current 0 [A])

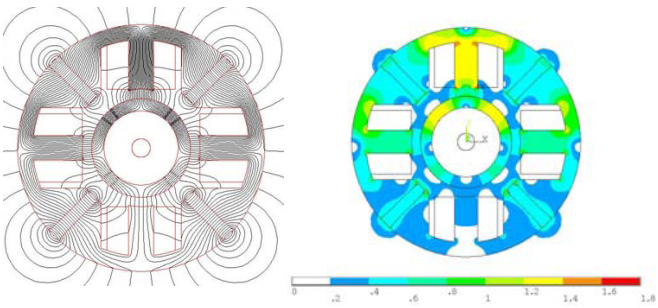

Figure 5. Flux lines and flux densities (Control current 2[A])

III. FEM Analysis and Design

The proposed magnetic bearing is designed through 2D EFM analysis. Analytical model and the parameters are shown in Fig. 3 and Table 1, respectively. Analytical flux lines and flux densities are shown in Fig. 4 (Control current 0[A]) and in Fig. 5 (Control current 2 [A]), respectively. Bias flux is well formed from the permanent magnets as shown in Fig. 4. When

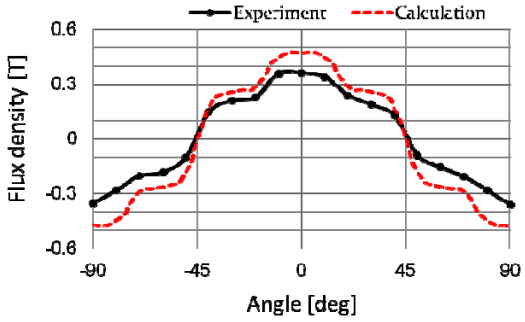

Figure 6. Flux densities in air gap

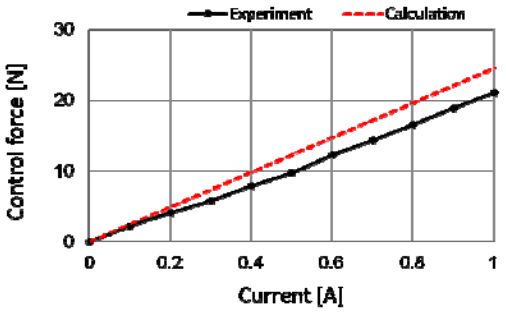

Figure 7. Control force characteristics

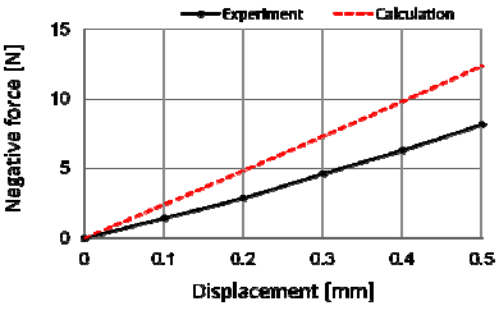

Figure 8. Negative force characteristics

the control current is 2 [A], the upper pole flux is near the saturation level around 1.3 [T] while the lower pole flux is lower than 0.1 [T] as shown in Fig. 5. Analyzed air gap flux density, control force and negative force characteristics are shown by the dotted red lines in Figs. 6, 7 and 8, respectively. The maximum bias flux of 0.48 [T], the control force factor of 26.1 [N/A] and the negaitve force factor of 25.4 [kN/m] are obtained from Figs. 6, 7 and 8, respectively. These values are considered enough high compared with the wide gap of 3 [mm]. These graphs also include the experimental results mentioned later.

IV. Experimental Setup and Static Characteristics

To confirm the capability of the proposed magnetic bearing the designed magnetic bearing is fablicated and tested. The desinged stator core and PM are shown in Fig. 9 while the photo of assembled stator is shown in Fig. 10. The stack thickness of the cores and PMs are 25 [mm].

The stator has PMs, control coils and sensors which produce electromagnetic flux change. The stator is better to be separated from the ultra-low temperature liquid. But any metal

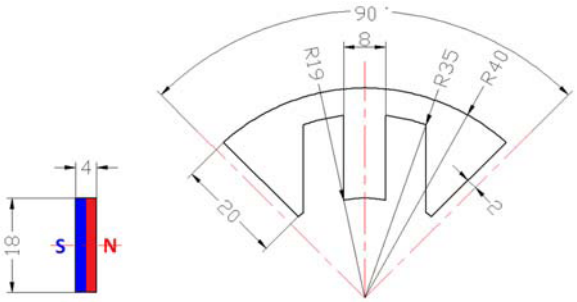

Figure 9. Designed stator core and permanent magnet

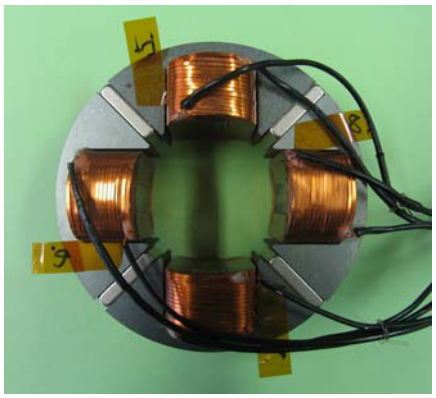

Figure 10. Photo of assembled stator

Figure 11. Fabricated magnetic bearing and flux density measurement

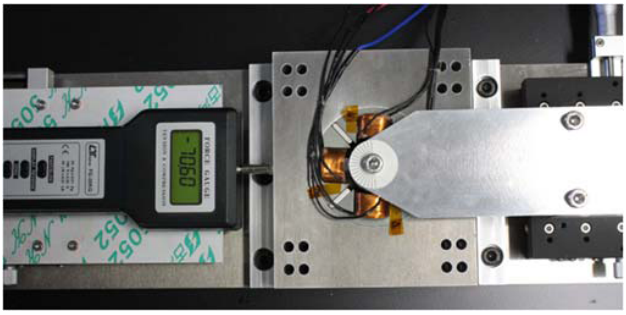

Figure 12. Photo of control and negative force measurement

can may affect adversly to dynamic change of flux. A special FRP pipe can be used in such low tempurature liqid which has 2 [mm] thickness [2]. The stator is designed to have 3 [mm] wide air gap.

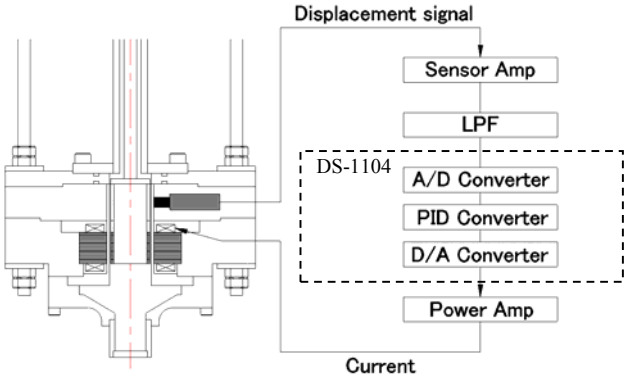

Figure 13. Schematic of control system

TABLE Ⅱ PID GAINS OF LEVITATION CONTRL

	Radial Value	
	$x-$direction	$y-$direction
K_P [A/m]	10	10
K_I [A·sec/m]	0.0001	0.0001
K_D [A/sec·m]	0.03	003

The flux density in air gap is measured by a gauss meter (Lake Shore 421, MNT-4E02-VH) as shown in Fig. 11. The fluxes of 10 [deg.] step are measured as shown by the dots with solid line in Fig. 6. The maximum flux density is about 0.36 [T] which is about 75 [%] of the calculated value. Also the control and the negative forces are measured by using the measuring setup as shown in Fig. 12. The measured control forces of 0.1 [A] step are shown by the dots with solid line in Figs. 7. Also the measured negative forces of 0.1 [mm] step are shown by the dots and solid line in Fig. 8. The force factor is about 21.1 [N/A] which is 88 [%] of the calculated one. The negative force factor is 16.4 [kN/m] which is 68 [%] of the calculated one. The measured values are lower than the calculated ones. This is mainly due to the 3 dimensional flux leakage which is not considered in 2D analysis. Even the measured values are lower than the calculated ones they are still high enough to control the pump.

V. CONTROL SYSTEM

For the levitation control we use dSPACE based PID digital controller. The control system is shown in Fig. 13. Radial x, y displacements are measured by eddy current sensors (AEC-5509) and put into the dSPACE (DS-1104) via third order anti-aliasing filter and A/D converter. The control gains are determined experimentally the values of which are shown in Table 2. Sampling interval used is $\tau - 0.1$ [ms] and the derivative time constant is 0.8 [ms]. The calculated actuating signal is put out through D/A converter to the analog power amplifier which is shown in Fig. 14. Thanks to high force factor of the proposed magnetic bearing the power amplifier consumes very low power.

VI. MAGNETICALLY LEVITATED PUMP

To confirm the developed magnetic bearing a simple pump test is carried out. The developed pump is shown in Fig. 15. This is planned to apply to the liqid nitrogen. However, water pumping is tested due to the university laboratory limitation.

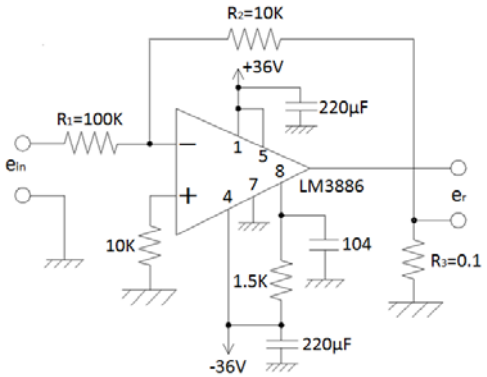

Figure 14. Power amplifier circuit

Figure 15. Photo of magnetically levitated pump

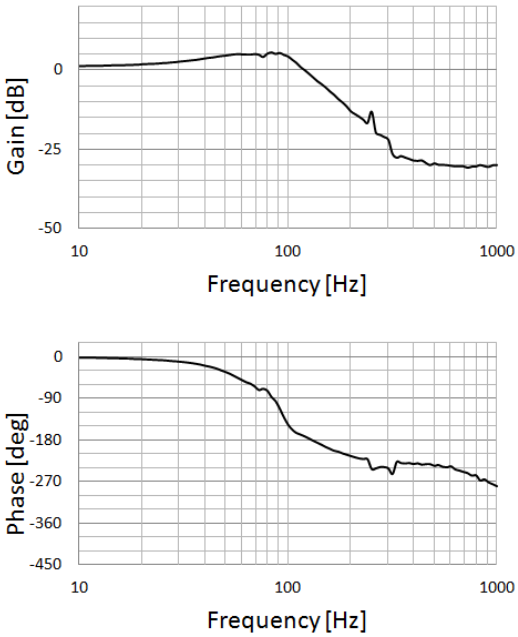

Figure 16. Frequency response in x-direction

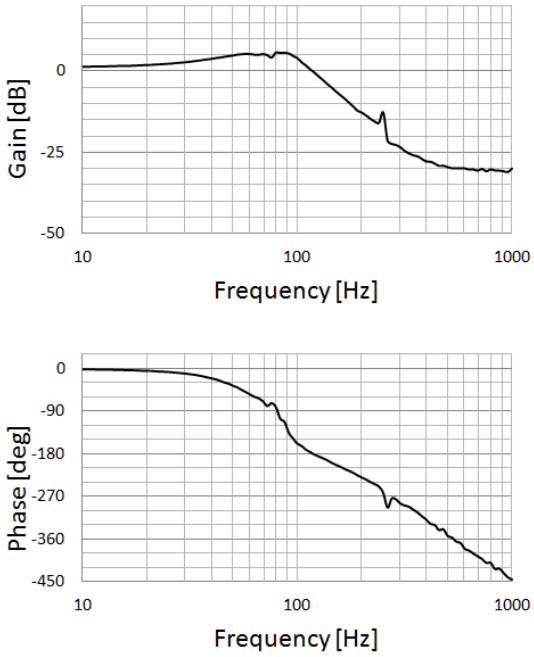

Figure 17. Frequency response in y-direction

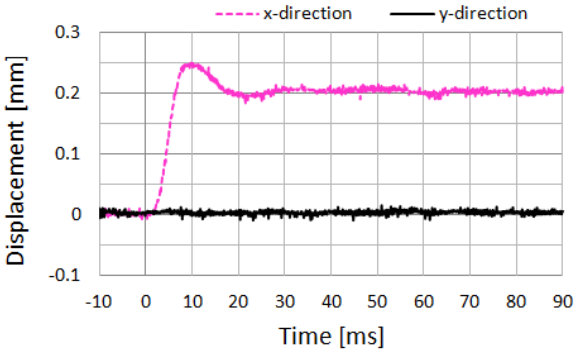

Figure 18. Step response (x-direction excitation)

As the same limitation the pumping pressure head is limited to 0.7 [m] while the actual pump has the nominal head of 8.7 [m]. Even the tested pressure is low the levitation of the pump is stable.

First the frequency responses are measured without rotation. The rotor is levitated with the filled water. The sinusoidal signal of ± 0.03 [mm] magnitude from 10 to 1000 [Hz] is put into the error signal and the corresponding levitated displacement is measured. The frequency response analyzer (NF FRA5095) is used for measurement. The responses of x- and y-directions are shown in Figs. 16 and 17, respectively. The maximum peak is about 5 [dB] around 85 [Hz]. The response is almost well reduced with PID controller except of the small peaks around 75 [Hz]. This is due to the poor support stiffness of the stator housing with narrow shafts. This might be improved by improving the support stiffness.

Next, the step response test is carried out. The signal of 0.2 [mm] is added to the error signal and the corresponding displacements are measured and recorded by the digital osciloscope (Yokogawa DL 708E). The x- and y-directional step responses are shown in Figs. 18 and 19, respectively.

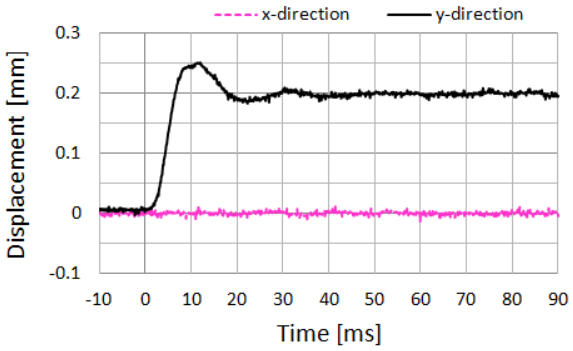

Figure 19. Step response (y-direction excitation)

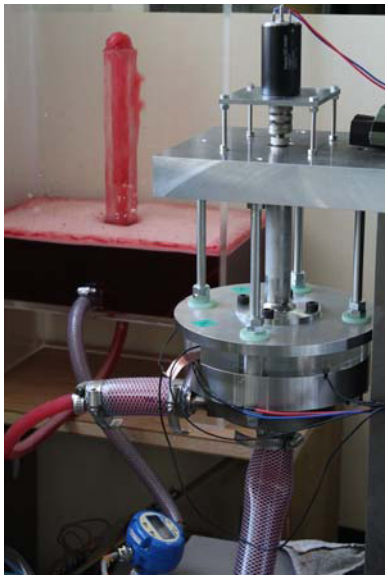

Figure 20. Photo of pumping test

Figure 18 is the x-directional excitation while Fig. 19 is the y-directional excitation. Both responses are well reduced within 30 [ms]. The cross coupling between x and y directions is not recognized in these responses.

VII. Pumping Test Results

Stable levitation is realized during the pumping test as shown in Fig. 20. The unbalance responses from 1,000 to 5,500 [rpm] are measured and the orbital trajectories are recorded as shown in Fig. 21. The levitated rotation is stable under the maxmum vibration of 60 [μm]. From these responses the x- and y-directional displacements are measured and recorded as shown in Fig. 22. The displacements are well controlled by the proposed PID controller. The flow rate versus rotating speed is shown in Fig. 23 while the x- and y-directional power consumptions of magnetic bearing are shown in Fig. 24. The nominal flow rate of 12 [L/min.] is recorded about the rotating speed of 2500 [rpm]. Vibration level is under 60 [μm] up to 5500 [rpm]. The x- and y-directional power consumptions of magnetic bearings are lower than 1.3 [W]. This means the high capability of the developed magnetic bearing to apply to the ultra-low temperature fluid pump.

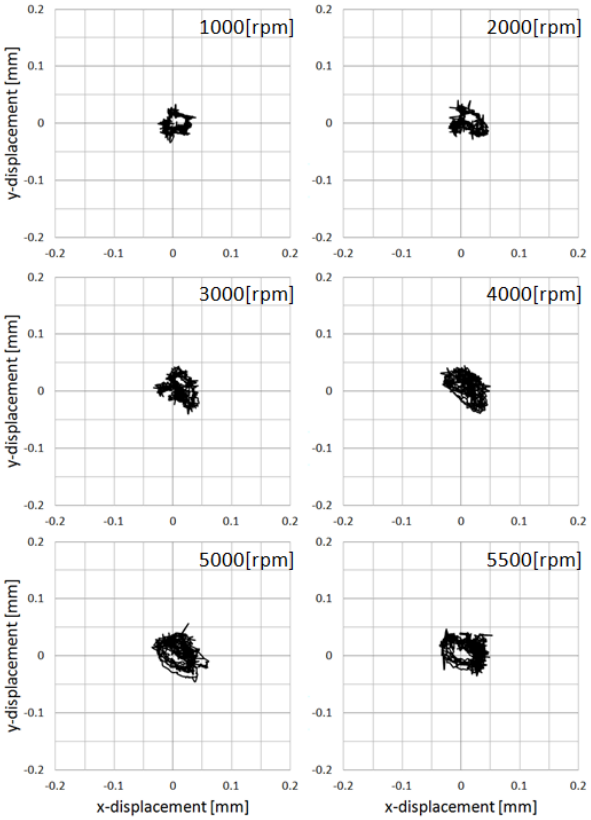

Figure 21. Orbital trajectory during pumping test

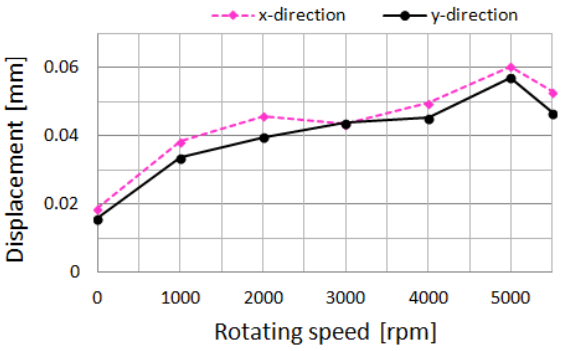

Figure 22. Vibration amplitude during orbital trajectory measument

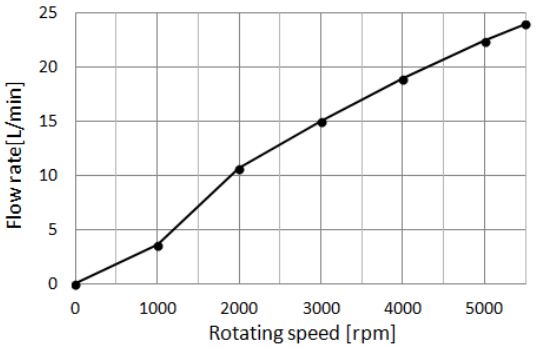

Figure 23 Flow rate versus rotating speed

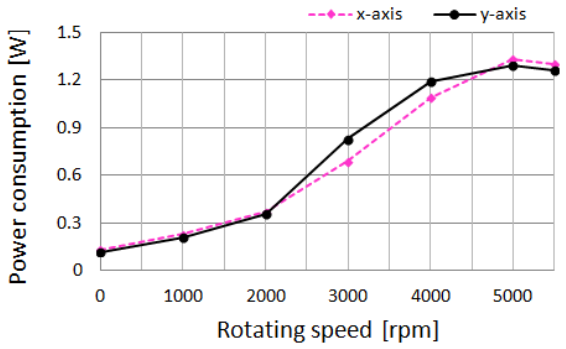

Figure 24 Power consumption of magnetic bearings versus rotating speed

VIII. Concluding Remarks

In this paper highly efficient magnetic bearing is developed which is planned to apply to ultra-low temperature fluid pump. The developed magnetic bearing can support the pump impeller successfully up to 5500 [rpm] over the rated operating speed of 3200 [rpm]. The power consumption recorded is very low level. Further research work is continuing to apply the developed pump to high pressure output and actual fluid such as liquid nitrogen or liquid helium.

Acknowledgement

This work is supported by Oita Prefecture Collaboration of Regional Entities for Advancement of Technology Excellence, JST.

References

[1] G. Schweitzer and E. H. Maslen, ed., "Magnetic Bearings", Springer, 2009.

[2] http://www32.ocn.ne.jp/~kfjhr/

[3] K. Kakihara, Y. Okada, and H. Koyanagi, "Development of IPM type Hybrid Magnetic Bearing", *Proc. of 6th Korea-Japan Symposium of Frontiers in Vibration Science and Technology*, Hitachi JAPAN, pp. 32-35, 2005.

[4] S. Kodama, et. al., "Development of 5 DOF IPM Type Magnetic Bearing", *CD-ROM Proc. of 8th Int. Conf. on Motion and Vibration Control*, KAIST, Daejeon, Korea, pp. 1-6, 2006.

[5] R. Martin, et. al., "Development of A Low Cost Permanent Magnet Biased Bearing", *CD-ROM Proc. of 9th Int. Symp. on Magnetic Bearings*, Lexington, Kentucky, USA, pp.1-6, 2004.

[6] K. Kakihara, Y. Otsuka, N. Kurita, and Y. Okada, "Development of Wide-Gap Hybrid Magnetic Bearing", *CD-ROM Proc. of 8th Int. Conf. on Motion and Vibration Control*, KAIST, Daejeon, Korea, pp. 1-6, 2006.

[7] Y. Okada, K. Sagawa, E. Suzuki, and R. Kondo, "Development and Application of Parallel PM type Hybrid Magnetic Bearings", *JSME Journal of System Design and Dynamics*, pp.1-10, 2009.

[8] H. Miyazawa, Y. Okada, R. Kondo, and M. Enokizono, "Development of a Flux Concentrated PM Type Magnetic Bearings", *Proc. of First Japan-Korea Joint Symposium on Dynamics and Control,* Sapporo JAPAN, pp. 183-186, 2009.

[9] Y. Okada, H. Miyazawa, R. Kondo, and M. Enokizono, "Proposal of Flux Concentrated Radial and Axial Magnetic Bearings", *Applied Electromagnetic Engineering, Edited by A. G. Mamalis, M. Enokizono, and A. Kladas,* Trans Tech Publications LTD, pp. 435-446, 2011.

[10] http://selco-coil.com/